Synthesis and Characterization of Oligonucleotides Containing a 4′-Keto Abasic Site†

Jingyang Chen‡ and JoAnne Stubbe*,‡,§

Departments of Chemistry and Biology, Massachusetts Institute of Technology, Cambridge, Massachusetts 02139

Received March 3, 2004

ABSTRACT: DNA strand breaks can result as a direct or indirect consequence of oxidative damage to the nucleic acid bases and/or deoxyribose sugars. Ionizing radiation and the antitumor agents, the bleomycins (BLMs) and enediynes, share in common the ability to indirectly cause DNA strand scission after C4′ hydrogen atom abstraction from the deoxyribose moiety. In the case of extensively studied BLMs, the C4′ radical generated under anaerobic conditions results in production of a 4′-keto abasic site after C4′ oxidation to a cation and H_2O addition. To study the structure, stability, and repair of this lesion, a general method is reported for its homogeneous preparation in any sequence context. 4′-Azido-2′-deoxyuridine-5′-triphosphate is incorporated into duplex DNA using a primer, a template containing a restriction enzyme (NgoM IV) cleavage site at its 3′-end, and HIV-1 reverse transcriptase. The two strands of the duplex are separated based on size after cleavage with the restriction enzyme. The single-stranded (ss) DNA containing 4′-azido-2′-deoxyuridine, when treated with uracil-DNA glycosylase, results in quantitative release of uracil, azide, and generation of a ss-DNA containing the 4′-keto abasic site. This lesion is characterized directly by MALDI-TOF MS and indirectly by subsequent reduction, enzymatic digestion, and GC/MS. The stability of duplex DNA containing a 4′-keto abasic site relative to an abasic site in the same sequence context is reported under physiological conditions.

Oxidative damage of DNA generates a wide range of lesions on the nucleic acid bases and the deoxyribose sugars that, if left unrepaired, results in mutations and ultimately disease (*1*). Most of the work in this area has focused on base lesions (*2*−*4*). However, it is estimated that 10−20% of the damage is associated with the deoxyribose backbone, and subsequently, frank or indirect DNA strand cleavage (*5*, *6*). The structures of a number of oxidatively damaged sugars resulting from ionizing radiation (*7*, *8*), chemical oxidants (*9*), and a variety of antitumor agents (*10*) have been characterized. The recent development of more sensitive analytical and mass spectrometric methods suggest that additional sugar damage will likely be identified, a requirement to understand the physiological consequences of the lesions and the mechanisms of their repair (*11*).

Our laboratory has been interested in the bleomycins (BLMs),[1] natural products used clinically in combination with other drugs in the treatment of a variety of cancers (*12*). The cytotoxicity of the BLMs is thought to be related to their ability to bind to duplex DNA and generate both single-stranded (ss) and double-stranded (ds) DNA lesions via oxidative damage to the deoxyribose backbone (*13*, *14*). Recent studies have also suggested that RNA may be a target of the BLMs (*15*). Cleavage of either DNA or RNA requires the presence of both ferrous iron and O_2, the cofactors thought to be required for BLM's activity in vivo. The difficulty in repairing the ds-lesions has suggested that they are predominantly responsible for the therapeutic efficacy of the BLMs (*16*, *17*). The sugar damage generated by BLMs is initiated by 4′-hydrogen atom abstraction from a pyrimidine 3′ to a guanine (*18*). The resulting 4′-radical can lead to two types of damage depending on the availability of O_2 (Scheme 1). Under anaerobic conditions, a 4′-keto abasic site is generated, which remains part of an intact DNA strand (*19*, *20*). In the presence of O_2, a 4′-peroxy radical is generated that eventually leads to a gapped 3′-phosphoglycolate/5′-phosphate lesion (3′-PG/5′-P) and elimination of a pyrimidine propenal (base propenal, Scheme 1) (*21*). The chemistry of this process is complex and slow (*19*, *22*). Both types of lesions are also generated by ionizing radiation and by other natural products such as the enediynes (*23*). Our laboratory's interest in the mechanism of cytotoxicity of the BLMs has recently led us to develop synthetic methods to make gapped 3′-PG/5′-P lesions and to study their structures by 2-D NMR methods (*24*). Generation of these lesions in any sequence context and knowledge of their structure should facilitate our understanding of the mechanism of recognition by DNA repair enzymes. We now report, using a combina-

† Supported by NIH Grant GM 34454 to J.S.

* Corresponding author. Tel: (617) 253-1814. Fax: (617) 258-7247. E-mail: stubbe@mit.edu.

‡ Department of Chemistry.

§ Department of Biology.

[1] Abbreviations: BLM, bleomycin; ss, single-stranded; ds, double-stranded; 3′-PG/5′-P, 3′-phosphoglycolate/5′-phosphate lesion; PAGE, polyacrylamide gel electrophoresis; BSTFA, *N*,*O*-bis(trimethysilyl)-trifluoroacetamide; TMCS, trimethylchlorosilane; TCEP, tris-(2-carboxyethyl)-phosphine; UDG, uracil-DNA glycosylase; AP, alkaline phosphatase; RT, reverse transcriptase; PDE-1: phosphodiesterase-1; FDH, formate dehydrogenase; RP-HPLC, reverse phase HPLC; MALDI, matrix-assisted laser desorption/ionization; 4′-N_3-dU, 4′-azido-2′-deoxyuridine.

10.1021/bi0495376 CCC: $27.50
Published on Web 04/14/2004

Scheme 1

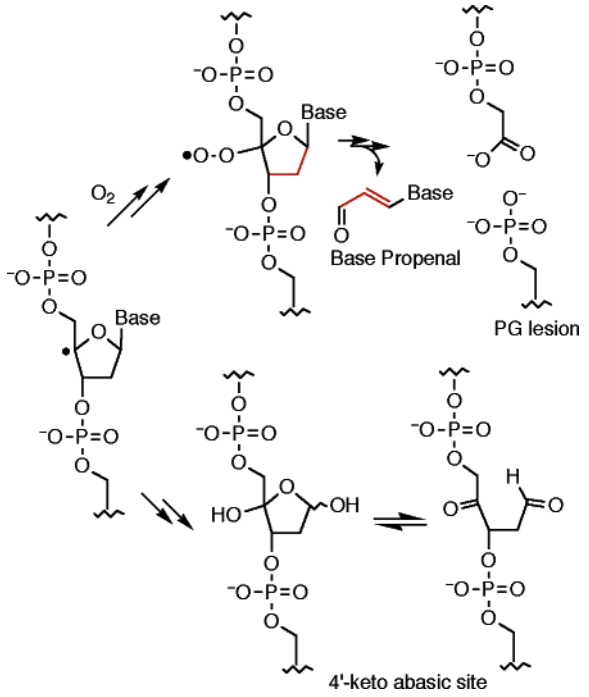

tion of synthetic and enzymatic methods (Figure 1), a convenient synthesis of the 4′-keto abasic site lesion and the preliminary characterization of its stability.

MATERIALS AND METHODS

The oligonucleotides (**2**−**4**, Table 1) were synthesized at the MIT Biopolymers Laboratory. Compounds **3** and **4** were purified by polyacrylamide gel electrophoresis (PAGE) (*25*). The following extinction coefficients (ϵ_{260}) were calculated as reported (*26*): **1**, 124.3 mM^{-1} cm^{-1}; **2**, 132.5 mM^{-1} cm^{-1}; **3**, 144.8 mM^{-1} cm^{-1}; **4**, 274.0 mM^{-1} cm^{-1}; **5**, 333 mM^{-1} cm^{-1}; **6**, 210 mM^{-1} cm^{-1}; **7**, 201 mM^{-1} cm^{-1}; and **8** or **9**, 242 mM^{-1} cm^{-1}. *N*,*O*-bis(trimethysilyl)trifluoroacetamide (BSTFA), trimethylchlorosilane (TMCS), and tris-(2-carboxyethyl)-phosphine (TCEP) were purchased from Pierce. All other chemicals were purchased from Sigma-Aldrich Co.

Escherichia coli uracil-DNA glycosylase (UDG, 1 U releases 60 pmol of uracil per minute from ds-uracil-containing DNA), DNA polymerase I−Klenow fragment (1 U converts 10 nmol of dNTPs to an acid-insoluble form in 30 min at 37 °C), and NgoM IV (1 U digests 1 μg of adenovirus-2 DNA in 1 h at 37 °C) were purchased from New England Biolabs. Alternatively, UDG was purified from expression plasmid pET21a-UDG kindly supplied by Dr. James Stivers, Johns Hopkins University, as previously described (*27*). Nuclease P1 (1 U catalyzes the hydrolysis of 1 μmol of phosphodiester linkage in yeast RNA in 1 min at 37 °C) and alkaline phosphatase from calf intestine (AP, 1 U catalyzes the hydrolysis of 1 μmol of 4-nitrophenyl phosphate in 1 min at 37 °C) were purchased from Roche. HIV-1 reverse transcriptase (HIV-1 RT, 1 U incorporates 1 nmol of dNTP in 20 min at 37 °C, pH 8.3) and snake venom phosphodiesterase-1 (PDE-1, 1 U hydrolyzes 1 μmol of *p*-nitrophenyl thymidine-5-phosphate in 1 min at 25 °C, pH 8.9) were purchased from Worthington Biochemical Co. Alternatively, HIV-1 RT was purified following the published protocol (*28*) from *E. coli* DH5α containing the p66-(his)/51 plasmid (*29*) (provided by Drs. Paul Boyer and Stephen Hughes, National Cancer Institute). AMV reverse transcriptase (AMV RT, 1 U incorporates 1 nmol of TMP into acid-insoluble product in 10 min at 37 °C) was purchased from USB. RAV-2 reverse transcriptase (RAV-2 RT, 1 U incorporates 1 nmol of TMP into acid-insoluble product in 10 min at 37 °C with poly (rA)/polyT as the primer/template) was purchased from Amersham Pharmacia Biotech. Human

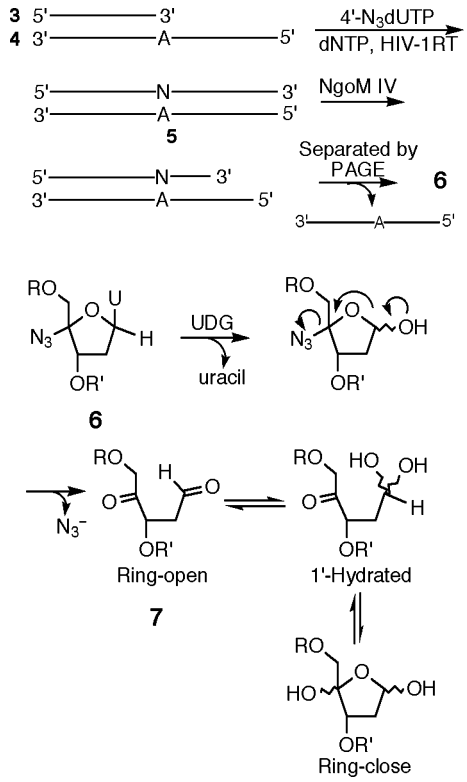

FIGURE 1: Synthesis of a 4′-keto abasic site lesion from 4′-N_3-dUTP using HIV-1 RT and UDG. The sequences of **3**−**7** are listed in Table 1. N: 4′-N_3-dU.

Table 1: Sequences of the Oligonucleotides Used in This Study[a]

	Sequence information *
1	5′-AAA AXA AAA-3′
2	5′-AAA AUA AAA-3′
3	5′-CTG AGC TCC AAA G-3′
4	5′-CTG CCG GCC CGG TAC TTT GGA GCT CAG-3′
5	5′-CTG AGC TCC AAA GNA CCG G⇓GC CGG CAG-3′ 3′-GAC TCG AGG TTT CAT GGC C⇑CG GCC GTC-5′
6	5′-CTG AGC TCC AAA GNA CCG GG-3′
7	5′-CTG AGC TCC AAA GYA CCG GG-3′
8	5′-CTG AGC TCC AAA GYA CCG GG-3′ 3′-GAC TCG AGG TTT CAT GGC CC-5′
9	5′-CTG AGC TCC AAA GXA CCG GG-3′ 3′-GAC TCG AGG TTT CAT GGC CC-5′

[a] *X: a normal abasic site. N: 4′-N_3-dU. Y: a 4′-keto abasic site. The underlined sequence denotes the NgoM IV recognition sequence, and ⇓ indicates the cleavage site.

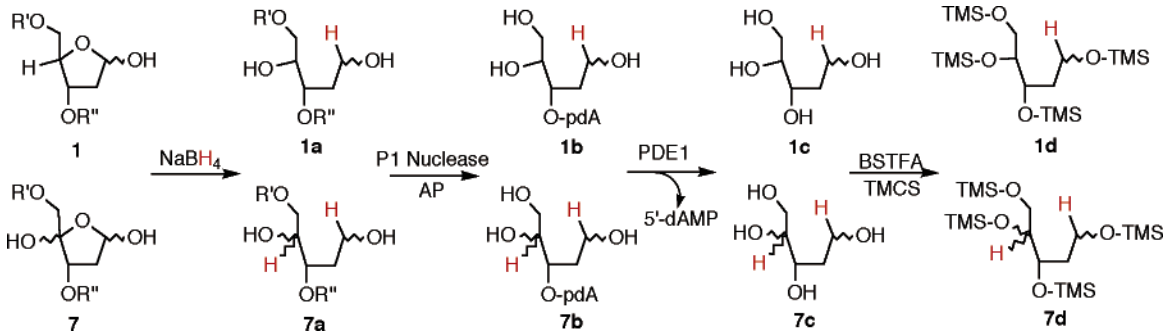

FIGURE 2: Characterization of oligonucleotides containing an abasic site (**1**) or a 4′-keto abasic site (**7**) by enzymatic digestion followed by GC/MS. Similar experiments have been performed with $NaBD_4$. Compounds **1d** and **7d** were subjected to GC/ MS analysis.

polymerase β (1 U incorporates 1 nmol of dNTP into acid-insoluble product in 1 h at 37 °C) was purchased from Trevigen. Yeast formate dehydrogenase (FDH, 1 U oxidizes 1.0 μmol of formate to CO_2 per min using at pH 7.5, 37 °C) was purchased from Sigma.

Ethanol precipitation of oligonucleotides was carried out in a volume of 1 mL by adding 0.3 M sodium acetate, pH 5.2 and 71.4% (v/v) ethanol. The mixture was incubated at −80 °C for 1 h and was centrifuged at 10 000*g* for 30 min. The supernatant was decanted, and the pellet was washed with 500 μL of ice-cold 75% ethanol. The mixture was centrifuged again at 10 000*g* for 30 min. The supernatant was removed, and the pellet was dried in vacuo.

Reverse phase HPLC (RP-HPLC) was carried out using a Nucleotide−Nucleoside Column (Alltech, 250 × 4.6 mm). Two different chromatographic elution programs were used. The first (system A) involved solution A (50 mM ammonium acetate, pH 7.0) and solution B (methanol) using a linear gradient of 0−50% B over 30 min with a flow rate of 1 mL/min. The second (system B) involved solution A (60 mM $KHPO_4$, 5 mM tetrabutylammonium phosphate, pH 4.7) and solution B (5 mM tetrabutylammonium phosphate in methanol) using a linear gradient of 0−50% B over 20 min and 50−90% over an additional 10 min with a flow rate of 1 mL/min.

Anion-exchange HPLC was carried out using a DNAPac 100 column (Dionex, 250 × 4 mm). The elution (system C) involved solution A (25 mM HEPES, pH 8.0) and solution B (200 mM $NaClO_4$, 25 mM HEPES, pH 8.0) using a linear gradient of 25−100% B over 15 min with a flow rate of 1 mL/min.

The GC/MS experiments were carried out on a Hewlett-Packard Agilent 5973N with an HP Restek Rtx-1 column (30 m × 250 μm × 1 μm). The oven temperature was maintained at 100 °C for 5 min followed by a linear gradient of 100−250 °C over the next 15 min.

Matrix-assisted laser desorption/ionization (MALDI)-mass spectrometry (MS) experiments were carried out on a Bruker Daltonics OminiFlex MALDI-TOF mass spectrometer. The MALDI matrix solution was prepared by mixing 2 volumes of 52.5 mg/mL 3-hydroxyl-picolinic acid in 50% acetonitrile/water (v/v) with 1 volume of 0.1 M diammonium citrate. Samples containing ∼200 pmol of oligonucleotide were loaded onto 10 μL of C18 ZipTip (MilliPore) and were desalted by washing twice with 20 μL of H_2O. The desalted oligonucleotides were eluted with 1 μL of MALDI matrix solution and were spotted on the target. The instrumental parameters were ion source 1, 19 kV; ion source 2, 17 kV; lens, 8.6 kV; extraction time, 200 ns; and sample rate, 1 per ns. The detector was set in a linear, positive mode.

*Synthesis of 5′-AAA AXA AAA-3′ (**1**, X Denotes an Abasic Site) as a Control.* Compound **1** (Table 1) was synthesized by treating crude 5′-AAA AUA AAA-3′ (**2**) with UDG. The reaction mixture contained in a final volume of 200 μL: 178 nmol of **2**, 20 mM Tris-HCl (pH 8.0), 1 mM EDTA, 1 mM DTT, and 100 U of UDG. The reaction was allowed to proceed at 37 °C for 4.5 h. Compound **1** was purified by RP-HPLC system A. (Compound, retention time, yield: uracil, 7.8 min, 114 nmol; **1**, 20.2 min, 110 nmol).

*Reduction of **1** to **1a** by $NaBH_4$ or $NaBD_4$ and Enzymatic Digestion of **1a** with Nuclease P1 and AP (Figure 2).* Compound **1** (20 nmol) was incubated with 50 mM $NaBH_4$ in 100 mM Tris-HCl (pH 8.3), in a total volume of 200 μL at 4 °C for 30 min. Acetic acid (20 μL) was added to neutralize the reaction mixture, and **1a** was separated by RP-HPLC system A. (Compound, retention time, yield: **1a**, 20.3 min, 19.2 nmol).

Nuclease P1 digestion of **1a** was carried out in a final volume of 100 μL containing 15 nmol of **1a**, 0.1 M NaOAc, pH 5.3, 0.1 mM $ZnCl_2$, and 15 U of nuclease P1. The reaction mixture was incubated at 37 °C for 1 h. The mixture was then diluted to 200 μL containing 50 mM Tris-HCl (pH 8.5), 0.1 mM EDTA, and 20 U of AP. The incubation was carried out at 37 °C for 30 min. The reaction was stopped when the reaction mixture was heated at 95 °C for 10 min. The protein was removed by centrifugation, and the products were separated by RP-HPLC system A to give the compound, retention time, and yield: **1b**, 17.4 min, 12 nmol; dA, 21.0 min, 85 nmol. Alternatively, the products of the enzymatic digestion of **1a** (5 nmol) were analyzed by RP-HPLC system B to give the compound, retention time, and yield: dA, 14.9 min, 27.4 nmol; **1b**, 19.1min, 4.3 nmol.

The reduction of **1** by $NaBD_4$ and the subsequent enzymatic digestion were carried out under the same conditions as described previously. The ESI-MS ($[M - H]^-$) for **1b** ($NaBH_4$): calcd 448.1239, found 448.1231; **1b** ($NaBD_4$): calcd 449.1302, found 449.1301.

*GC/MS Analysis of 2-Deoxy-pentitols (**1c**) Derived from **1b**.* Compound **1b** (8 nmol) was incubated in 50 mM Tris-HCl (pH 8.3), 10 mM $MgCl_2$, and 2 U of PDE-1 in a total volume of 20 μL. The reaction was allowed to proceed at 37 °C for 2 h. The reaction was stopped when the reaction mixture was heated at 95 °C for 10 min. The protein was removed by centrifugation. Half of the reaction mixture was subjected to RP-HPLC (system B), and the product was found to coelute with 5′-dAMP. The other half was lyophi-

lized and transferred to a 0.3 mL reaction vial (Pierce) by being dissolved in methanol followed by evaporating to dryness in vacuo. Compound **1c** (4 nmol) was silylated with a 20 μL of 1:1 acetonitrile/BSTFA (with 1% TMCS) at 100 °C for 30 min to produce **1d** (Figure 2). An aliquot (1 μL) of the silylation mixture was then analyzed by GC/MS. Compound **1d** was eluted at 17.4 min (224 °C). (MS spectrum in Figure S1, Supporting Information.)

Synthesis of 4′-Azido-2′-deoxyuridine-5′-monophosphate (4′-N_3-dUMP). 4′-Azido-2′-deoxyuridine (4′-N_3-dU) was synthesized as previously reported (*30*). It was converted to 4′-N_3-dUMP using a modification of the method of Yoshikawa et al. (*31*). 4′-N_3-dU (50 mg, 0.186 mmol) was dissolved in 0.5 mL of freshly distilled triethyl phosphate. Freshly distilled $POCl_3$ (74.6 μL, 0.80 mmol) was then added dropwise with stirring at 4 °C. The reaction mixture was slowly warmed to room temperature and stirred for an additional 12 h. The mixture was then diluted into 50 mL of ice-cold water and titrated with NaOH until the pH was between 7 and 7.5.

The 4′-N_3-dUMP was purified on a DEAE Sephadex A-25 column (2.5 × 22 cm) using a linear gradient of 0−0.4 M triethylammonium bicarbonate (TEAB, 1 × 1 L). The flow rate was 2.7 mL/min, and the fraction size was 28 mL. 4′-N_3-dUMP eluted at 0.25 M TEAB, and the fractions were pooled and concentrated in vacuo until the triethylamine was removed. The product was characterized by ^{1}H NMR: (D_2O, HDO = 4.81 ppm, δ): 2.48 (2H, m, H2′/H2″), 4.09 (2H, m, H5′/H5″), 4.59 (1H, m, H3′), 5.81 (1H, d, J = 7.9 Hz, H5), 6.33 (1H, m, H1′), 7.71 (1H, d, J = 7.9 Hz, H6). The overall yield was 50%.

Synthesis of 4′-Azido-2′-deoxyuridine-5′-triphosphate (4′-N_3-dUTP). 4′-N_3-dUTP was prepared from 4′-N_3-dUMP via the method by Hoard and Ott (*32*). 4′-N_3-dUMP (34 μmol) was dissolved in 0.5 mL of DMF, and tributylamine (8.1 μL, 34 μmol) was added. The solvent was removed in vacuo, and the salt was rendered anhydrous by evaporation with dry DMF (4 × 0.25 mL), dry pyridine (2 × 0.25 mL), and dry DMF (2 × 0.25 mL). The resulting product was then dissolved in 0.3 mL of DMF, and 27.5 mg of 1,1′-carbonyldiimidazole (171 μmol) in 0.3 mL of DMF was added. The reaction mixture was stirred for 12 h at room temperature under argon. Then, 9.8 μL of H_2O/DMF (1:1) was added, and the reaction mixture was stirred for another 30 min at room temperature. Tributylammonium pyrophosphate (169.9 μmol) in 2 mL of DMF was added, and the reaction mixture was stirred for an additional 24 h. The supernatant was collected, and the precipitate was washed 5 times with 0.5 mL of DMF. The combined supernatant and washes were mixed with 5 mL of methanol, and the solvent was removed in vacuo. The pellet was dissolved in 15 mL of cold water. The product was purified on a DEAE Sephadex A-25 column (2.5 × 15 cm) with a linear gradient (0.65 × 0.65 L, 0−0.8 M) of TEAB. The flow rate was 3 mL/min, and the fraction size was 17.5 mL. The major peak eluted at 0.6−0.68 M TEAB. The fractions were pooled and concentrated in vacuo. The product was characterized by ^{1}H NMR (D_2O, HDO = 4.81 ppm, δ): 2.52 (2H, m, H2′/H2″), 4.25 (2 H, m, H5′/H5″), 4.83 (1 H, m, H3′), 5.93 (1 H, d, J = 8.1 Hz, H5), 6.42 (1 H, m, H1′), 7.85 (1 H, d, J = 8.1 Hz, H6). The yield of 4′-N_3-dUTP was 50%.

Incorporation of 4′-N_3-dU into Duplex DNA using a Primer Extension Method. The reaction mixture contained the following in a final volume of 1 mL: 10 μM primer (**3**, Table 1), 10 μM template (**4**, Table 1), 1 mM dNTPs (dATP, dGTP, and dCTP), 0.1 mM 4′-N_3-dUTP, 50 mM Tris-HCl (pH 8.3), 50 mM KCl, 10 mM $MgCl_2$, 0.5 mM DTT, and 300 U of HIV-1 RT. Compounds **3** and **4** were annealed by heating at 100 °C for 5 min followed by cooling to room temperature over 1 h before dNTPs and HIV-1 RT were added. The reaction mixture was incubated at 37 °C, and the reaction was monitored using [5′-^{32}P]-**3**. Aliquots were taken (2 μL) at various incubation times and analyzed by a 12% sequencing gel (35 × 42 cm). The gel was run at constant power of 90 W for 3 h and was then dried, exposed to a storage phosphor screen (Molecular Dynamics, now Amersham Biosciences), and visualized on a Storm 840 PhosphorImager (Molecular Dynamics, now Amersham Biosciences). The reaction was complete in 2 h, and the product, **5**, was separated from the reaction mixture by ethanol precipitation.

*Isolation of ss-Oligonucleotide Containing 4′-N_3-dU (**6**, Table 1) from ds-**5**.* ss-DNA is required for UDG to remove uracil from 4′-N_3-dU. Compound **5** was designed with an NgoM IV restriction site (Table 1). The reaction mixture of 200 μL contained **5** (5 nmol) and 120 U of NgoM IV in a buffer (50 mM potassium acetate, 20 mM Tris-acetate, 10 mM magnesium acetate, and 1 mM DTT, pH 7.9) and was incubated at 37 °C for 12 h. Compound **6** (Table 1, 20mer) was separated from its complimentary strand (24mer) on a 12% polyacrylamide gel (20 × 20 cm) at constant voltage of 350 V for 2 h. The gel was visualized by UV shadow. Compound **6** was recovered from the gel in 50% yield.

*Removal of Uracil from **6** using UDG.* The reaction mixture of 160 μL contained 10 μM **6**, 160 U of UDG, 20 mM HEPES, pH 8.0, and 1 mM EDTA. The reaction was incubated at 37 °C, and uracil release was monitored by RP-HPLC system A (compound, retention time: uracil, 7.8 min; **6**, 23.0 min; and **7**, 21.5 min). The reaction was completed in 2 h.

Quantitation of Azide Release using Formate Dehydrogenase (FDH). The release of azide was monitored using the procedure by Blanchard and Cleland (*33*). The assay mixture in 500 μL contained 1.7 mM sodium formate, 10 mM NAD^+, 100 mM HEPES (pH 7.5), and 0.025 U of FDH. The rate of the reaction was measured by change in A_{340nm} (ϵ = 6.2 mM^{-1} cm^{-1}). A standard curve was generated by the addition of various amounts of azide (50−200 nM) to the reaction mixture, and the decrease in rate was plotted against the azide concentration. To quantitate the azide release during the conversion of **6** to **7**, **6** (3.2 nmol) was treated with UDG under the conditions described previously. The reaction mixture was analyzed by RP-HPLC system A. Uracil was quantitated, and the flow-through of the column (retention time 2.5−3.5 min, 1 mL) was collected. Aliquots were added to the FDH assay mixture, and the azide concentration was quantitated by the inhibition based on the standard curve.

*Reduction of **7** to **7a** by $NaBH_4$ or $NaBD_4$ and Digestion of **7a** by Nuclease P1 and AP (Figure 2).* **7** (2.2 nmol) was reduced by $NaBH_4$ under the conditions described previously

for the abasic site control. The reaction mixture was neutralized by addition of 20 μL of acetic acid, and the reduced product, **7a**, was purified by RP-HPLC system A to give the compound, retention time, yield: **7a**, 21.7 min, 2.0 nmol.

Compound **7a** was then digested by nuclease P1 and AP as described previously (Figure 2). Compound **7b** has a retention time identical to thymidine using RP-HPLC system A. Therefore, **7b** was isolated using ion-pairing RP-HPLC (system B). Compound **7b** was lyophilized and desalted using RP-HPLC system A. Its retention times were identical to **1b** in both RP-HPLC systems A and B. The reduction of **7** by $NaBD_4$ and the subsequent enzymatic digestion were carried out under the same conditions as described previously.

*Conversion of **7b** to 2-Deoxypentitol (**7c**) and 5′-dAMP Followed by GC/MS Analysis.* Compound **7b** (2.0 nmol) was digested with PDE-1 and silylated to give **7d** as described previously for the abasic site oligonucleotide. Compound **7d** was eluted at 17.4 min (224 °C).

*Stability of the Duplex DNA (**8**) Containing a 4′-Keto Abasic Site.* Compound **8** (10 μM) was generated by annealing **7** with its complementary strand in 100 mM NaCl and 10 mM sodium phosphate (pH 7.0) at 70 °C for 1 min followed by cooling to 20 °C in a heat block over 1 h. Compound **8** was incubated at 37 °C, and aliquots were analyzed by anion-exchange HPLC at 10 h intervals from 0 to 70 h. The stability of the abasic site lesion (**9**, Table 1) in the same sequence context was monitored under identical conditions.

RESULTS

Incorporation of 4′-N_3-dU into Duplex DNA. Two general methods have been developed to incorporate nucleotide analogues into oligonucleotides. The most widely used strategy is generation of the appropriately blocked phosphoramidite of the unnatural nucleoside and use of solid-phase DNA synthesis methods (*34*) to generate ss-DNA. The second requires chemical synthesis of the nucleoside 5′-triphosphate analogues and use of a primer/template and a DNA polymerase to make duplex DNA. The latter method is often required when the nucleotide analogue phosphoramidites are unstable to the solid-phase methods. Both approaches have been reported for incorporation of 4′-azidothymine into oligonucleotides. Gibson et al. reported the synthesis of 4′-azidothymidine phosphoramidite and its incorporation into ss-DNA by the standard solid-phase DNA synthesis method (*35*). Unfortunately, the starting material, 4′-azidothymidine phosphoramidite, and the final oligonucleotide product were characterized. In our hands, 4′-N_3-dU is not stable to the concentrated ammonia conditions required to remove oligonucleotide from the solid support (unpublished result). Therefore, this approach for incorporation of 4′-N_3-dU into DNA is problematic.

The studies of Chen et al. showing that 4′-azidothymidine-5′-triphosphate can be incorporated into duplex DNA using HIV-1 reverse transcriptase (*36*) suggested that the primer/template/polymerase approach for incorporation of 4′-N_3-dU would be successful. Incorporation of unnatural nucleotides using polymerases often encounters problems with either slow incorporation or slow extension after incorporation. Recently, the simultaneous use of two DNA polymerases has been applied to overcome these shortcomings (*37*).

Scheme 2

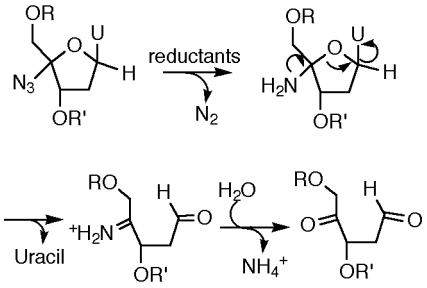

We investigated a number of DNA polymerases (including Klenow fragment, AMV RT, human DNA polymerase β, RAV-2 RT, and HIV-1 RT) for their efficiency of incorporation of 4′-N_3-dUTP and extension into duplex DNA. The Klenow fragment failed to incorporate 4′-N_3-dUTP under all conditions. AMV RT could incorporate 4′-N_3-dU; however, the extension resulted in significant amounts of truncated products. Human DNA polymerase β, RAV-2 RT, and HIV-1 RT were all found to incorporate 4′-N_3-dUTP and to generate complete duplex DNA. In the reaction catalyzed by DNA polymerase β, however, product degradation was observed due to the requirement of DTT and high pH (pH 8.8) for enzyme activity. Under these conditions, the azide was reduced by DTT, generating the 4′-keto abasic site (Scheme 2). At pH 8.8, this intermediate underwent phosphodiester bond cleavage. Lowering pH or removing DTT greatly reduced the efficiency of polymerase β. The ability to isolate large amounts of HIV-1 RT from an overexpression system and its efficiency at incorporation and extension to generate intact duplex DNA was the basis for our choice of HIV-1 RT for further studies.

Using [5′-^{32}P]-(**3**) as the primer and **4** as the template (Table 1), the time dependent incorporation of 4′-N_3-dUTP into an oligonucleotide by HIV-1 RT was monitored by PAGE (Figure 3). The gel reveals some stalling in extension of the primer after the incorporation of 4′-N_3-dU. However, in 2 h, all of the primer can readily be converted to product (Figure 4, lane 2). The overall yield of **5** was 95%. The actual primer extension product is one nucleotide longer than the template due to the terminal nucleotide addition activity of HIV-1 RT (Figure 3, lane 6) (*38*).

*Isolation of **6** from 5 (Figure 1).* Our strategy to generate 4′-keto abasic site is shown in Figure 1. The key step is to use UDG to remove uracil, generating a 4′-azido abasic site intermediate that we predicted would rapidly lose azide to generate the desired lesion. Previous studies of Lindahl and Stivers have demonstrated that both ss- and ds-DNA containing deoxyuridine are substrates of UDG with ss-DNA being hydrolyzed 20 times more efficiently than ds-DNA (*39*, *40*). Our efforts to use UDG to convert 4′-N_3-dU to a 4′-keto abasic site in duplex DNA, however, were unsuccessful. No uracil release was observed even with 150 000 times the amount of enzyme used in the cleavage of uracil from deoxyuridine and extended incubation times. Thus, to use UDG to release uracil, we needed to separate the two strands of the duplex. To achieve this separation, one end of the duplex DNA (**5**) was designed to contain an NgoM IV

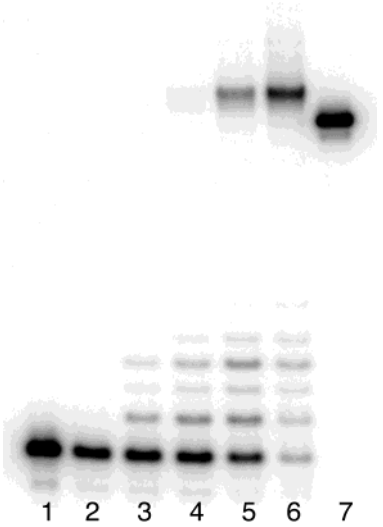

FIGURE 3: Monitoring incorporation of 4′-N_3dU into duplex DNA using primer [5′-^{32}P]-**3** and template **4** with HIV-1 reverse transcriptase. Lane 1: [5′-^{32}P]-**3** (13mer); lanes 2−6: 0, 10, 20, 30, and 60 min incubation time; lane 7: [5′-^{32}P]-27mer as a MW marker. At 2 h, all stalled oligonucleotides were converted to product (see Figure 4).

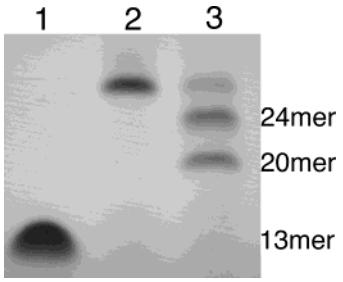

FIGURE 4: Denaturing PAGE allows separation of ss-DNA containing 4′-N_3dU from its complement after treatment of the duplex DNA with NgoM IV. Lane 1: The primer (**3**) only. Lane 2: The primer extension reaction mixture containing the intact duplex (**5**), which is a 27mer. Lane 3: The two ss-DNA fragments generated by restriction enzyme digestion: a 24mer and one 20mer (**6**).

cleavage site (Table 1). Digestion of the duplex with this restriction endonuclease resulted in production of two oligonucleotides: a 24mer and the desired 20mer (**6**). The size difference was sufficient for strand separation using denaturing PAGE. The bands were visualized by a UV shadow as shown in Figure 4. Compound **6** was purified from the gel by the crush and soak method (*25*) in 50% overall recovery. NgoM IV digestion also eliminated the variable end of the extended primer, present due to HIV-1 RT's nontemplated nucleotide addition activity. The MALDI-TOF MS analysis of **6** showed $[M + H]^+$: 6155.65 (calculated: 6154.97). To further characterize **6**, it was digested with nuclease P1 and AP. The resulting nucleosides were analyzed by RP-HPLC system A, giving ratios of dC/dG/T/4′-N_3-dU/dA as 5.5:6:2.1:1.1:4.9, consistent with the expected ratios (6:6:2:1:5, Figure 5).

*Conversion of **6** into a 4′-Keto Abasic Site Containing Oligonucleotide (**7**) by UDG.* The isolated ss-**6** was incubated with UDG to determine whether the desired 4′-keto abasic site containing oligonucleotide (**7**) could be generated. Uracil release, monitored by HPLC (Figure S2, Supporting Information), was quantitative. However, the amount of UDG required for efficient uracil release was 3000-fold greater than that used to quantitatively generate uracil from deoxyuridine in the same sequence context. The product, **7**, was analyzed by MALDI-MS. The $[M + H]^+$ observed was 6033.21, suggesting that the product is a ring-closed or -opened 1′-hydrated aldehyde (calcd: 6033.03). No ring-opened, unhydrated species (calcd: 6015.02) was detected. Previous studies examining an abasic site labeled at C1′ with ^{13}C and ^{17}O revealed that the aldehydic (ring-opened) form and its hydrate constituted less than 1% of total species, with the majority of the abasic site being a ring-closed mixture of α/β anomers (*41*, *42*). On the basis of the MALDI-MS analysis and these previous studies on the normal abasic site, we propose that the dominant form of **7** is the ring-closed hemiacetal.

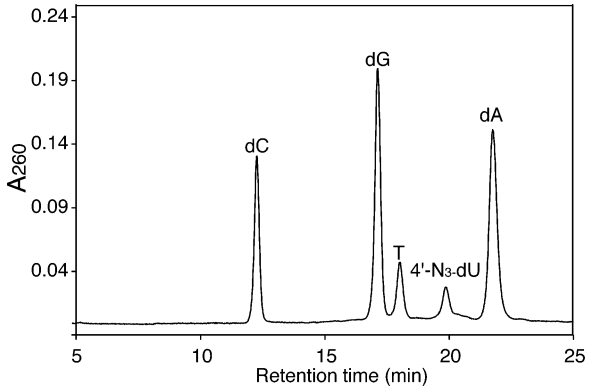

FIGURE 5: Characterization of **6** via digestion with nuclease P1 and AP followed by separation of the resulting nucleosides by RP HPLC (solvent system A).

*Characterization of a 4′-Keto Abasic Site Formation. Quantitation of Azide Release during the Conversion of **6** to **7**.* Our synthetic scheme (Figure 1) predicts that a stoichiometric amount of azide should accompany uracil release. Previous studies of Blanchard and Cleland have shown that azide is a potent inhibitor of formate dehydrogenase with $K_i = 7$ nM (*33*). A standard curve for azide inhibition of FDH was generated (Figure S3, Supporting Information). The flow-through of the RP-HPLC column was used in the FDH assay to quantitate the azide release. Comparison of inhibition caused by the azide in the flow-through relative to the standard curve revealed that azide and uracil were released in a 1:1 ratio.

*Enzymatic digestion of **7** and GC/MS Analysis of the Deoxypentitols (**7c**).* The structure of the 4′-keto abasic site (**7**) was further characterized as outlined in Figure 2 following the strategy of Rabow et al. (*20*). An abasic site standard (**1**) was characterized as a control for the sequence of reactions described in Figure 2. Compound **7** was converted to **7a** by reduction with $NaBH_4$ (or $NaBD_4$). Compound **7a** was enzymatically digested into its nucleoside components using Nuclease P1 and AP. The products were then analyzed by ion-pairing RP-HPLC (system B), giving ratios of dC/dG/T/dA/**7b** as 5.5:6.0:2.0:4.0:0.86, consistent with the expected ratios of 6:6:2:4:1 (Figure 6). Compound **7b** comigrated with an authentic sample of this species generated from the digestion of the abasic site control (**1b**, Figure 2).

To further support the structural assignment of **7b**, it was hydrolyzed by PDE-1 to produce 2-deoxypentitol (**7c**) and 5′-dAMP. Compound **7c** was silylated, and GC/MS analysis revealed two products (**7d)** associated with the diastereomers

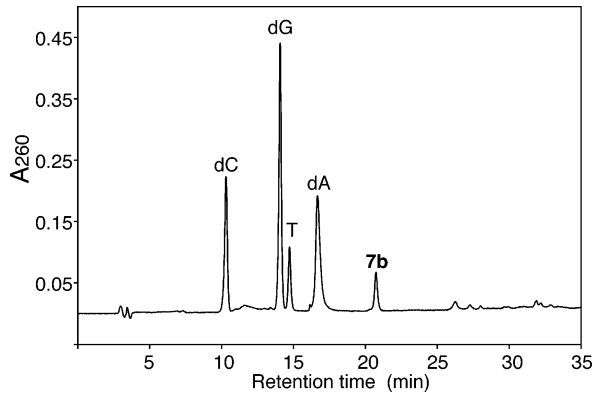

FIGURE 6: Ion-pairing RP-HPLC (system B) of the products generated when **7** was reduced by $NaBH_4$ followed by digestion with Nuclease P1 and AP.

resulting from reduction of the ketone at C4′. The mass spectrum of both products revealed a fragmentation pattern identical to that observed with **1d** (Figure S4, Supporting Information). The mass spectrum of $NaBD_4$ reduced **7d** unambiguously established the incorporation of two deuterium atoms: one at C1′ and the second at C4′. The MS data in conjunction with the degradation studies establish that the 4′-keto abasic site lesion can be generated in 50% yield from the starting primer/template.

*Stability of a Duplex DNA (**8**) Containing a 4′-Keto Abasic Site Relative to an Abasic Site in the Same Sequence Context (**9**).* As with abasic sites, 4′-keto abasic sites are also chemically labile. The ring opened, aldehydic form of this compound has been proposed to be susceptible to elimination of the 3′-phosphate, and consequently, DNA strand scission (*13*). A preliminary experiment was carried out to examine the stability of this lesion under conditions that mimic physiological pH and ionic strength. The elimination process was monitored using anion-exchange chromatography under conditions in which the duplex DNA remained intact. The stability of the duplex DNA containing a normal abasic site (**9**, Table 1) in the same sequence context as **8** was also examined under the same conditions. The result establishes that the 4′-keto abasic site, which has a half-life of 26 h, is chemically more labile than the abasic site, which has a half-life of 130 h (Figure S5, Supporting Information).

DISCUSSION

4′-Keto abasic sites are common DNA lesions generated by ionizing radiation damage, the BLMs, and the enediynes. The preparation of these lesions has posed a synthetic challenge due to their chemical instability. During the preparation of this manuscript, Kim et al. reported a chemical synthesis of a phosphoramidite stable to standard solid-phase DNA synthesis, which upon photolysis, can generate a 4′-keto abasic site (*43*). We also have focused on the generation of a precursor to this lesion. After its incorporation into DNA, this precursor could be transformed into the desired lesion under mild conditions (either by reduction or enzymatically) to avoid the problem of DNA strand scission (Figure 1). As noted next, both methods provide a moderately facile route to this unstable lesion that will allow the detailed investigation of its chemical properties, structure, and the consequences of its generation in vivo.

The success of 3′-azido thymidine (AZT) as an AIDS therapeutic resulted in synthesis of a number of other azido modified nucleosides including 4′-azido nucleosides (*30*). These compounds appeared to be ideal precursors to the 4′-keto abasic site if a polymerase could be identified to catalyze their incorporation into DNA. Previous studies of Chen et al. (*36*) and recent studies with other unusual nucleotides (*44*, *45*) suggested that HIV-1 RT is sufficiently promiscuous not only to incorporate the modified nucleotides but also to catalyze chain extension to generate full-length duplex DNA. Once incorporated, several routes were envisioned that could lead to the desired product without phosphodiester bond cleavage. As noted previously, incorporation proceeds efficiently and quantitatively.

To examine the generation of the desired lesion, we first investigated reductants such as thiolates and water-soluble phosphines (*46*). Reduction of the 4′-azido group should result in the generation of a 4′-amine, which could potentially collapse to a 4′-imine abasic site (Scheme 2). The 4′-imine could then be hydrolyzed to a ketone and ammonia. Reduction proceeded rapidly with a variety of thiolates. Unfortunately, due to the basic conditions required to generate thiolates, the rate of phosphodiester bond cleavage was comparable to the rate of the azide reduction (unpublished data). This approach was consequently abandoned.

A water soluble phosphine, tris-(2-carboxyethyl)-phosphine (TCEP), was also examined as a potential reductant (*46*). The reduction proceeded rapidly and efficiently on 4′-N_3-dU. When this nucleoside was within the context of DNA, however, the rate of reduction was drastically reduced, presumably due to the electrostatic clash between the DNA and the carboxylate groups of TCEP. A noncharged water soluble phosphine should be successful and perhaps would allow direct reduction within the duplex.

Because of the difficulties associated with chemical reduction, the enzymatic conversion by UDG was investigated. This reaction leads directly to uracil release and subsequently azide release, generating the desired product (Figure 1). While previous studies have shown that both ss- and ds-DNA containing deoxyuridine are substrates of UDG, the reduced reactivity of 4′-N_3-dU with UDG has limited the substrate to ss-DNA. Despite this limitation, we are able to generate this lesion in vitro in quantities sufficient for structure determination and analysis with DNA repair enzymes.

Given the recent report of a phosphoramidite method to make a 4′-keto abasic site (*43*), a comparison of this method with our method is desirable. Both methods represent fairly lengthy syntheses. The light-mediated method involves a seven-step synthesis of the phosphoramidite precursor from deoxyribose with an overall yield of 9%. The mixture of 4′-diastereomers makes spectroscopic analysis of each synthetic step difficult. In addition, while no details of oligonucleotide synthesis were presented, a chain extension of the unnatural C4′ diastereomer is expected to be less efficient. Our synthesis also involves a seven-step synthesis from deoxyluridine to 4′-N_3-dUTP with an overall 10% yield. The incorporation of 4′-N_3-dU and its conversion to the 4′-keto abasic site resulted in 50% yield. The most inefficient step is the isolation of ss-DNA via PAGE. Recently, the use of a biotin-tagged template DNA has been developed to remove this problem, resulting in very high recoveries (unpublished data).

The half-life of a 4′-keto abasic site was also measured by Kim et al. and found to be 7.8 h (37 °C, 100 mM NaCl at pH 7.5) in ss-DNA (*43*). The rate constant is faster by a factor of 3 relative to the one we have measured in ds-DNA (26 h at 37 °C, 100 mM NaCl at pH 7). Although the pH conditions and the sequences are different in the two studies, we believe duplex DNA stabilizes the lesion. A similar effect of DNA structure has recently been reported for the 2-deoxyribonolactone abasic site lesion (*47*). Its half-life was found to be 20 h in ss-DNA and 32−54 h in ds-DNA (37 °C, 150 mM NaCl, 2 mM $MgCl_2$ at pH 7.5) (*47*). Stability of sugar lesions, not surprisingly, appears to be sensitive to both sequence and sequence context (ss vs ds).

Finally, it is desirable to generate the 4′-keto abasic site in duplex DNA. We believe it is likely that a single diastereomer at C-4′ might result, constrained by the duplex structure. It will be important to compare this structure with those generated from ss-DNA. Only the former structure is likely to be physiologically significant. As noted previously, our method, thus far, has failed to directly generate the lesion in duplex DNA. It has not been reported whether the photolysis method can generate this lesion in duplex DNA. In our case, we are hopeful that, given the availability of a variety of 4′-azido-substituted deoxynucleotides (U, G, T, A, and C) (*30*), mismatch repair DNA glycosylases will allow generation of 4′-keto abasic sites in duplex DNA (*48*). If one of these enzymatic approaches is successful, the lesion could be generated in vivo, which is not possible by the light-mediated approach.

Oxidative damage occurs to both the bases and the sugars of DNA (*1*). Damage to the bases and the mutagenic consequences of this damage have been much more extensively investigated (*2*−*4*) than damage to the deoxyribose sugars. Previous studies have been reported on the generation of 4′-keto abasic sites using BLM (Scheme 1) (*49*, *50*). Unfortunately, the cleavage of DNA by BLMs is not very sequence-specific, and consequently, generation of the 4′-keto abasic site at the primary site also results in lesions at secondary sites. The difficulty of preparing this lesion homogeneously using BLMs has thus limited its examination with DNA repair enzymes. Studies of Demple et al. on a 36mer containing a single 4′-keto abasic site generated with BLM have demonstrated that Ape1 can catalyze phosphodiester bond cleavage 5′ to the lesion, resulting in a 3′-OH end and a 5′-phosphorylated-lesioned deoxyribose (*49*). Although a detailed kinetic analysis was not carried out, the efficiency of cleavage was suggested to be similar to Ape1 catalyzed reaction on an abasic site. Recently, using the phosphoramidite approach, the 4′-keto abasic site has been studied with a variety of DNA polymerases (*51*). Our ability to generate the 4′-keto abasic site lesion and the 3′-PG/5′-P lesion in any sequence context should now allow us to understand the structure of the lesions (both ss- and ds-lesions) and the efficiency with which they are repaired by Ape1 and β-polymerase and to further characterize other repair proteins.

ACKNOWLEDGMENT

We thank Naoko Abe for technical assistance and Dr. Manas Ghorai for synthesizing 4′-N_3-dUTP. We also thank Dr. James Stivers for providing pET21a-UDG, an overexpression system for uracil glycosylase and the purification procedure, and Drs. Paul Boyer and Stephen Hughes for providing HIV-1 RT expression plasmid p66(his)/51.

SUPPORTING INFORMATION AVAILABLE

Figures showing MS spectra of **1d** and **7d**, HPLC traces of conversion of **6** to **7**, quantitation of azide release, and measurement of the half-life of **8** by anion-exchange HPLC. This material is available free of charge via the Internet at http://pubs.acs.org.

REFERENCES

1. Demple, B., and Harrison, L. (1994) Repair of oxidative damage to DNA: Enzymology and Biology, *Annu. Rev. Biochem. 63*, 915−948.
2. Cadet, J., D'Ham, C., Douki, T., Pouget, J. P., Ravanat, J. L., and Sauvaigo, S. (1998) Facts and artifacts in the measurement of oxidative base damage to DNA, *Free Radical Res. 29*, 541−50.
3. Cadet, J., Bourdat, A. G., D'Ham, C., Duarte, V., Gasparutto, D., Romieu, A., and Ravanat, J. L. (2000) Oxidative base damage to DNA: specificity of base excision repair enzymes, *Mutat. Res. 462*, 121−8.
4. Mitra, S., Boldogh, I., Izumi, T., and Hazra, T. K. (2001) Complexities of the DNA base excision repair pathway for repair of oxidative DNA damage, *Environ. Mol. Mutagen. 38*, 180−90.
5. Deeble, D. J., Schulz, D., and von Sonntag, C. (1986) Reaction of OH radicals with poly(U) in deoxygenated solutions: sites of OH attack and the kinetics of base release, *Int. J. Radiat. Biol. 49*, 915−926.
6. von Sonntag, C. (1987) *The chemical basis of radiation biology*, Taylor and Francis, London.
7. Beesk, F., Dizdaroglu, M., Schulte-Frohlinde, D., and von Sonntag, C. (1979) Radiation-induced DNA strand breaks in deoxygenated aqueous solutions. The formation of altered sugars as end groups, *Int. J. Radiat. Biol. 36*, 565−76.
8. Hutchinson, F. (1985) Chemical changes induced in DNA by ionizing radiation, *Prog. Nucleic Acid Res. Mol. Biol. 32*, 115−54.
9. Breen, A. P., and Murphy, J. A. (1995) Reactions of oxyl radicals with DNA, *Free Radical Biol. Med. 18*, 1033−77.
10. Povirk, L. F., and Goldberg, I. H. (1987) Role of oxidative DNA sugar damage in mutagenesis by neocarzinostatin and bleomycin, *Biochimie 69*, 815−23.
11. Cadet, J., Douki, T., Gasparutto, D., and Ravanat, J. L. (2003) Oxidative damage to DNA: formation, measurement, and biochemical features, *Mutat. Res. 531*, 5−23.
12. Sikic, B. I., Rozencweig, M., and Carter, S. K. (1985) *Bleomycin Chemotherapy*, Academic Press, Orlando, FL.
13. Stubbe, J., and Kozarich, J. W. (1987) Mechanisms of bleomycin-induced DNA degradation, *Chem. Rev. 87*, 1107−1136.
14. Burger, R. M. (1998) Cleavage of nucleic acids by bleomycin, *Chem. Rev. 98*, 1153−1169.
15. Abraham, A. T., Lin, J. J., Newton, D. L., Rybak, S., and Hecht, S. M. (2003) RNA cleavage and inhibition of protein synthesis by bleomycin, *Chem. Biol. 10*, 45−52.
16. Povirk, L. F., Han, Y. H., and Steighner, R. J. (1989) Structure of Bleomycin-Induced DNA Double-Strand Breaks: Predominance of Blunt Ends and Single-Base 5′ Extensions, *Biochemistry 28*, 5809−5814.
17. Steighner, R. J., and Povirk, L. F. (1990) Bleomycin-induced DNA lesions at mutational hot spots: implications for the mechanism of double-strand cleavage, *Proc. Natl. Acad. Sci. U.S.A. 87*, 8350−8354.
18. Wu, J. C., Kozarich, J. W., and Stubbe, J. (1985) Mechanism of bleomycin: evidence for a rate-determining 4′-hydrogen abstraction from poly(dA-dU) associated with the formation of both free base and base propenal, *Biochemistry 24*, 7562−7568.
19. Sugiyama, H., Xu, C., Murugesan, N., and Hecht, S. M. (1985) Structure of the alkali-labile product formed during iron(II)-bleomycin-mediated DNA strand scission, *J. Am. Chem. Soc. 107*, 4101−4105.
20. Rabow, L. E., Stubbe, J., Kozarich, J. W., and Gerlt, J. A. (1986) Identification of the alkaline-labile product accompanying cytosine release during bleomycin-mediated degradation of d(CGCGCG), *J. Am. Chem. Soc. 108*, 7130−7131.

21. Burger, R. M., Berkowitz, A. R., Peisach, J., and Horwitz, S. B. (1980) Origin of malondialdehyde from DNA degraded by Fe(II)-bleomycin, *J. Biol. Chem. 255*, 11832−11838.
22. McGall, G. H., Rabow, L. E., Ashley, G. W., Wu, S. H., Kozarich, J. W., and Stubbe, J. (1992) New insight into the mechanism of base propenal formation during bleomycin-mediated DNA degradation, *J. Am. Chem. Soc. 114*, 4958−4967.
23. Dedon, P. C., and Goldberg, I. H. (1992) Free-radical mechanisms involved in the formation of sequence-dependent bistranded DNA lesions by the antitumor antibiotics bleomycin, neocarzinostatin, and calicheamicin, *Chem. Res. Toxicol. 5*, 311−332.
24. Junker, H. D., Hoehn, S. T., Bunt, R. C., Marathius, V., Chen, J., Turner, C. J., and Stubbe, J. (2002) Synthesis, characterization, and solution structure of tethered oligonucleotides containing an internal 3′-phosphoglycolate, 5′-phosphate gapped lesion, *Nucleic Acids Res. 30*, 5497−508.
25. Sambrook, J., Fritsch, E. F., and Maniatis, T. (1989) *Molecular Cloning: a Laboratory Manual*, 2nd ed., Cold Spring Harbor Laboratory Press, Plainview, NY.
26. Wallace, R. B., and Miyada, C. G. (1987) *Guide to Molecular Cloning Techniques*, Academic Press, New York.
27. Stivers, J. T., Pankiewicz, K. W., and Watanabe, K. A. (1999) Kinetic mechanism of damage site recognition and uracil flipping by *Escherichia coli* uracil DNA glycosylase, *Biochemistry 38*, 952−963.
28. Le Grice, S. F. J., Cameron, C. E., and Benkovic, S. J. (1995) Purification and characterization of human immunodeficiency virus Type 1 reverse transcriptase, *Methods Enzymol. 262*, 130−144.
29. Boyer, P. L., Tantillo, C., Jacobo-Molina, A., Nanni, R. G., Ding, J., Arnold, E., and Hughes, S. H. (1994) Sensitivity of wild-type human immunodeficiency virus type 1 reverse transcriptase to dideoxynucleotides depends on template length; the sensitivity of drug-resistant mutants does not, *Proc. Natl. Acad. Sci. U.S.A. 91*, 4882−6.
30. Maag, H., Ryszewski, R. M., McRoberts, M. J., Ruth-Crawford, D., Verheyden, J. P., and Prisbe, E. J. (1992) Synthesis and anti-HIV activity of 4′-azido and 4′-methoxynucleosides, *J. Med. Chem. 35*, 1440−1451.
31. Yoshikawa, M., Kato, T., and Takenishi, T. (1967) A novel method for phosphorylation of nucleosides to 5′-nucleotides, *Tetrahedron Lett. 50*, 5065−5068.
32. Hoard, D. E., and Ott, D. G. (1965) Conversion of mono- and oligodeoxyribonucleotides to 5′-triphosphates, *J. Am. Chem. Soc. 87*, 1875−1878.
33. Blanchard, J. S., and Cleland, W. W. (1980) Kinetic and chemical mechanisms of yeast formate dehydrogenase, *Biochemistry 19*, 3543−3550.
34. Caruthers, M. H. (1991) Chemical Synthesis of DNA and DNA Analogues, *Acc. Chem. Res. 24*, 278−284.
35. Gibson, N. J., McKellar, C. M., and Brown, T. (1996) The stability and conformation of duplex DNA containing the novel anti-HIV drug ADRT, *Biomed. Pept. Proteins Nucleic Acids 2*, 23−26.
36. Chen, M. S., Suttmann, R. T., Papp, E., Cannon, P. D., McRoberts, M. J., Bach, C., Copeland, W. C., and Wang, T. S. (1993) Selective action of 4′-azidothymidine triphosphate on reverse transcriptase of human immunodeficiency virus type 1 and human DNA polymerases _ and β, *Biochemistry 32*, 6002−10.
37. Tae, E. L., Wu, Y., Xia, G., Schultz, P. G., and Romesberg, F. E. (2001) Efforts toward expansion of the genetic alphabet: replication of DNA with three base pairs, *J. Am. Chem. Soc. 123*, 7439−7440.
38. Golinelli, M. P., and Hughes, S. H. (2002) Nontemplated nucleotide addition by HIV-1 reverse transcriptase, *Biochemistry 41*, 5894−5906.
39. Lindahl, T., Ljungquist, S., Siegert, W., Nyberg, B., and Sperens, B. (1977) DNA N-glycosidases: properties of uracil-DNA glycosidase from *Escherichia coli*, *J. Biol. Chem. 252*, 3286−3294.
40. Drohat, A. C., Jagadeesh, J., Ferguson, E., and Stivers, J. T. (1999) Role of electrophilic and general base catalysis in the mechanism of *Escherichia coli* uracil DNA glycosylase, *Biochemistry 38*, 11866−11875.
41. Manoharan, M., Ransom, S. C., Mazumder, A., Gerlt, J. A., Wilde, J. A., Withka, J. A., and Bolton, P. H. (1988) The characterization of abasic sites in DNA heteroduplexes by site specific labeling with ^{13}C, *J. Am. Chem. Soc. 110*, 1620−1622.
42. Wilde, J. A., Bolton, P. H., Mazumder, A., Manoharan, M., and Gerlt, J. A. (1989) Characterization of the equilibrating forms of the aldehydic abasic site in duplex DNA by ^{17}O NMR, *J. Am. Chem. Soc. 111*, 1894−1896.
43. Kim, J., Gil, J. M., and Greenberg, M. M. (2003) Synthesis and characterization of oligonucleotides containing the C4′-oxidized abasic site produced by bleomycin and other DNA damaging agents, *Angew. Chem., Int. Ed. 42*, 5882−5885.
44. Marx, A., Amacker, M., Stucki, M., Hubscher, U., Bickle, T. A., and Giese, B. (1998) 4′-Acylated thymidine 5′-triphosphates: a tool to increase selectivity towards HIV-1 reverse transcriptase, *Nucleic Acids Res. 26*, 4063−4067.
45. Marx, A., Spichty, M., Amacker, M., Schwitter, U., Hubscher, U., Bickle, T. A., Maga, G., and Giese, B. (1999) Probing interactions between HIV-1 reverse transcriptase and its DNA substrate with backbone-modified nucleotides, *Chem. Biol. 6*, 111−116.
46. Burns, J. A., Butler, J. C., Moran, J., and Whitesides, G. M. (1991) Selective reduction of disulfides by tris(2-carboxyethyl) phosphine, *J. Org. Chem. 56*, 2648−2650.
47. Zheng, Y., and Sheppard, T. L. (2004) Half-life and DNA strand scission products of 2-deoxyribonolactone oxidative DNA damage lesions, *Chem. Res. Toxicol. 17*, 197−207.
48. Scharer, O. D., and Jiricny, J. (2001) Recent progress in the biology, chemistry, and structural biology of DNA glycosylases, *Bioessays 23*, 270−281.
49. Xu, Y. J., Kim, E. Y., and Demple, B. (1998) Excision of C-4′-oxidized deoxyribose lesions from double-stranded DNA by human apurinic/ apyrimidinic endonuclease (Ape1 protein) and DNA polymerase β, *J. Biol. Chem. 273*, 28837−28844.
50. Povirk, L. F., and Houlgrave, C. W. (1988) Effect of apurinic/ apyrimidic endonucleases and polyamines on DNA treated with bleomycin and neocarzinostatin: specific formation and cleavage of closely opposed lesions in complementary strands, *Biochemistry 27*, 3850−3857.
51. Greenberg, M. M., Weledji, Y. N., Kroeger, K. M., Kim, J., and Goodman, M. F. (2004) In vitro effects of a C4′-oxidized abasic site on DNA polymerases, *Biochemistry 44*, 2656−2663.

BI0495376